KAVLI INSTITUTE 7/24/2007

SPATIAL FIELD AND INTENSITY CORRELATIONS IN QUASI-ONE-DIMENSIONAL GEOMETRIES

Gabriel Cwilich

Yeshiva University

More details in: Phys Rev E, 045603(R) , 2006

Luis S. Froufe Perez Ecole Centrale, Paris

Juan Jose Saenz Univ. Autonoma, Madrid

THANK YOU DON and HERB

KAVLI Institute

Where is Yeshiva University ?

OUTLINE

- Coherent transport
- Diagrammatic theory
- Correlations
- Experimental motivation
- Transport Random Matrix Theory
- Numerical Results
- Conclusions

Wave transport in a disordered system:

A brief review of the diagrammatic theory

Gabriel Cwilich

Department of Physics

Yeshiva University

PHYSICAL REVIEW VOLUME 109, NUMBER 5 MARCH 1, 1958

Absence of Diffusion in Certain Random Lattices

P. W. ANDERSON
Bell Telephone Laboratories, Murray Hill, New Jersey
(Received October 10, 1957)

This paper presents a simple model for such processes as spin diffusion or conduction in the "impurity band." These processes involve transport in a lattice which is in some sense random, and in them diffusion is expected to take place via quantum jumps between localized sites. In this simple model the essential randomness is introduced by requiring the energy to vary randomly from site to site. It is shown that at low enough densities no diffusion at all can take place, and the criteria for transport to occur are given.

VOLUME 16, NUMBER 22 PHYSICAL REVIEW LETTERS 30 MAY 1966

BREAKDOWN OF THE CONCENTRATION EXPANSION FOR THE IMPURITY RESISTIVITY OF METALS*

J. S. Langer and T. Neal†
Carnegie Institute of Technology, Pittsburgh, Pennsylvania
(Received 18 April 1966)

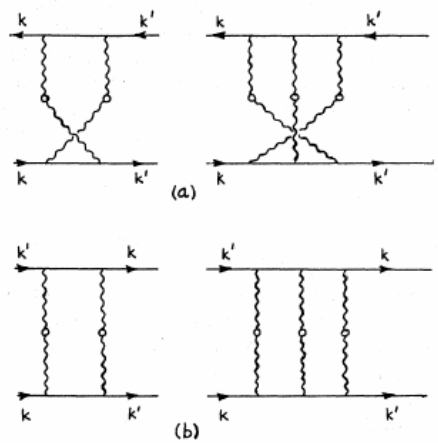

Propagation of classical waves in disordered systems

"scrambling" of the signal

Loss of information

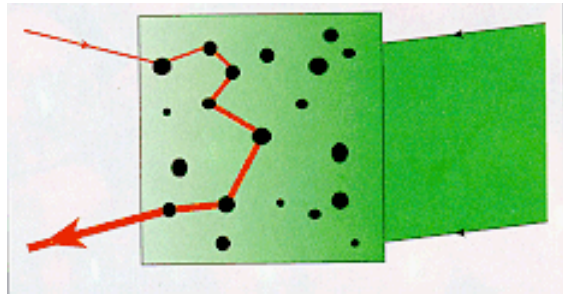

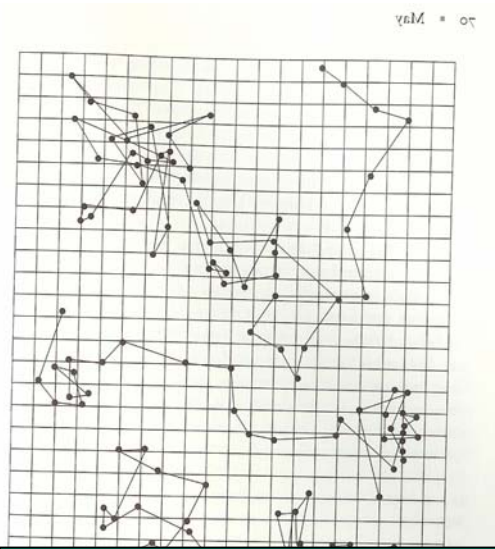

COHERENT PROPAGATION

Coherent backscattering

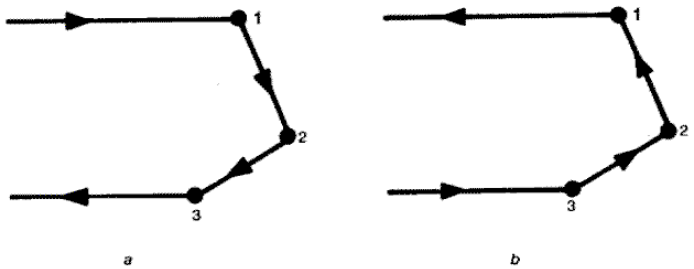

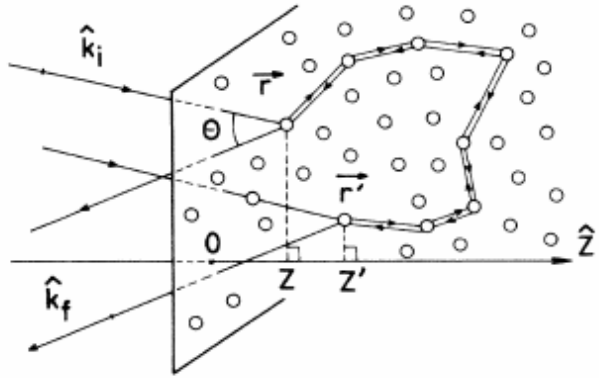

Something survives after averaging over disorder

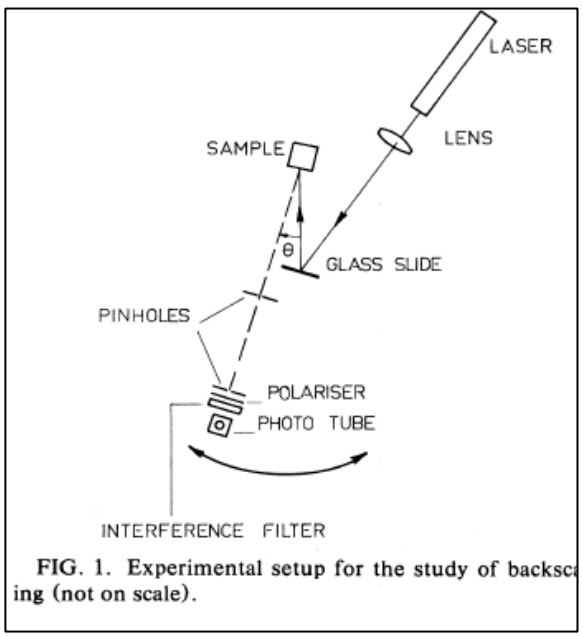

FIG. 1. Experimental setup for the study of backsca ing (not on scale).

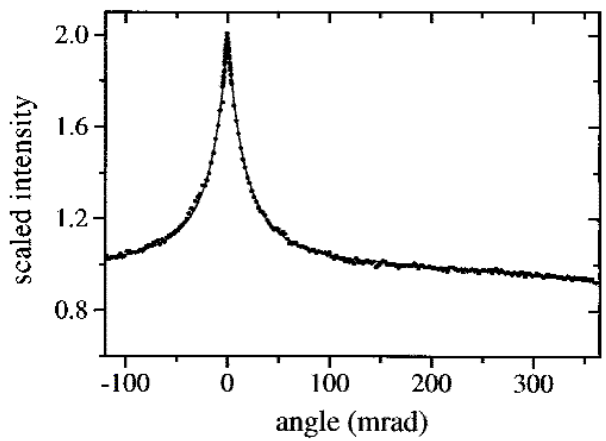

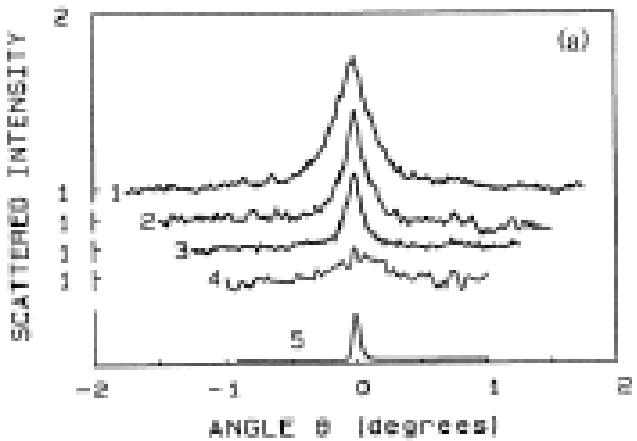

FIG. 3. (a) Dependence of the coherent backscattering effect on the solid fraction (n) of beads: curve 1, $n = 0.11$; curve 2, $n = 0.06$; curve 3, $n = 0.026$; and curve 4, $n = 0.004$. The bead diameter is 0.46 μm. The analyzer is parallel to the vertical incident polarization, VV. For each curve, the intensity is normalized to the incoherent background intensity (i.e., the intensity outside the peak). Curve

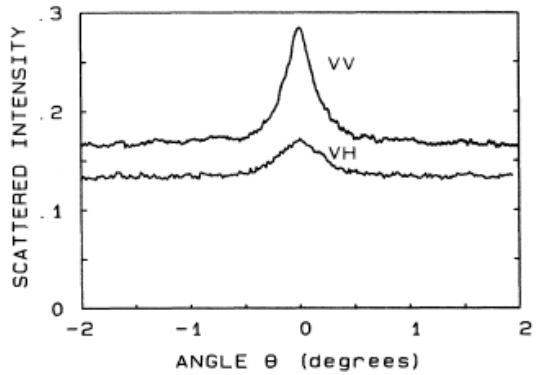

FIG. 4. Polarization dependence of the coherent backscattering effect for 0.46-μm-diam beads at a solid fraction of 10%. Directions of polarization are vertical-vertical (VV) and vertical-horizontal (VH). Curves are plotted at the same scale.

$\ell < L < \ell_{inc}$

(many collisions, phase is preserved)

Quantum transport. Or rather coherent transport.

No quantum statistics.

Information about the system

Width, polarization.

Diffusive Wave spectroscopy

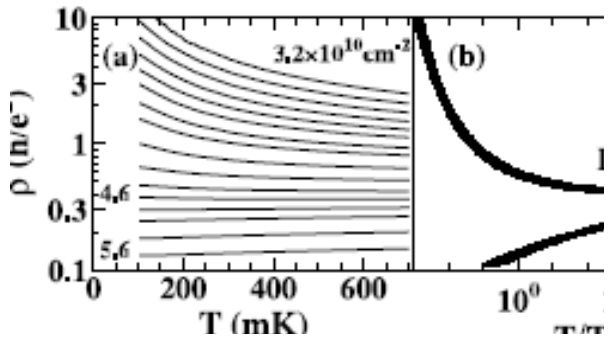

Breaking the phase coherence between the time-reversed paths

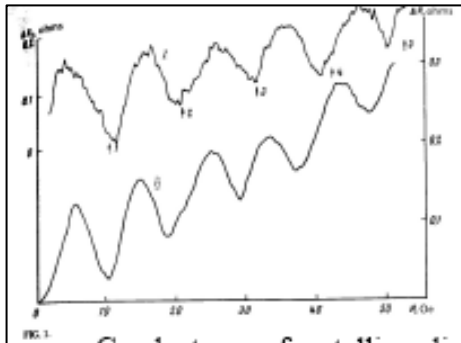

Sharvin & Sharvin (1981)

Conductance of metallic cylinders *vs* magnetic field:
$\Phi_0 / 2$ - oscillations

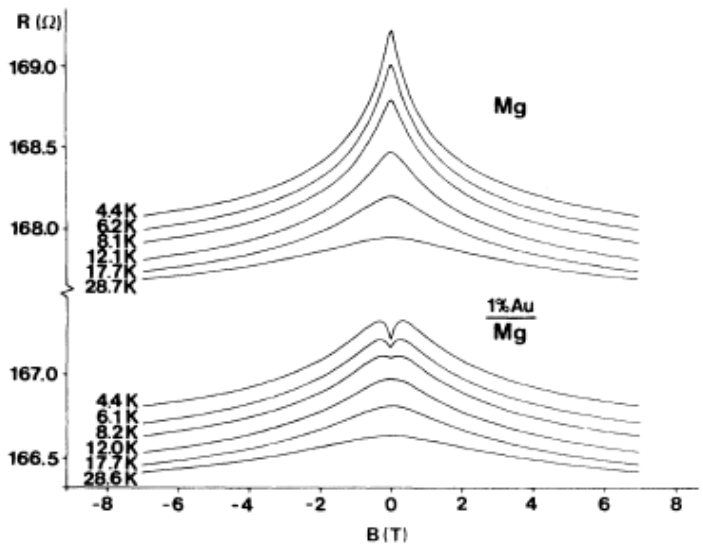

FIG. 6. Magnetoresistance of a pure Mg film at different temperatures (upper part). A superposition of $\frac{1}{100}$ atomic layer of Au (statistically) changes the behavior completely. The Au introduces a rather pronounced spin-orbit coupling which rotates the spins of the complementary scattered waves. This changes the interference from constructive to destructive.

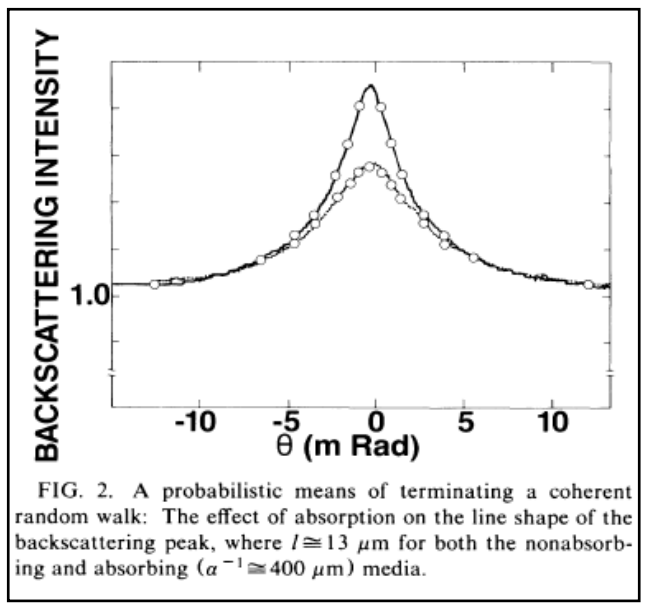

FIG. 2. A probabilistic means of terminating a coherent random walk: The effect of absorption on the line shape of the backscattering peak, where $l \cong 13\ \mu$m for both the nonabsorbing and absorbing ($\alpha^{-1} \cong 400\ \mu$m) media.

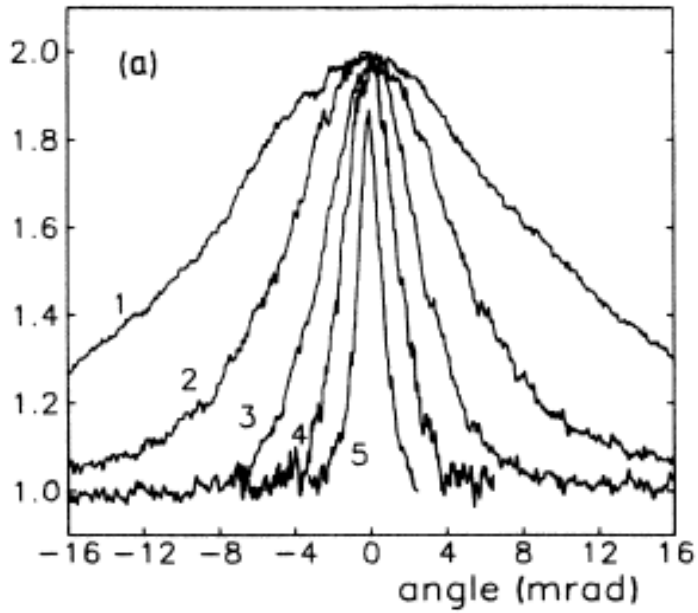

FIG. 20. (a) Normalized (see text) difference cones recorded for the parallel light component using the sample of Fig. 19. Difference slabs: curve 1, 0–13 μm; curve 2, 13–25 μm; curve 3, 25–50 μm; curve 4, 50–100 μm; curve 5, 100–1000 μm. (b)

NOTE: In typical optical experiments we measure average quantities.

Phenomena at many scales

- Electronic systems (a few atoms)
- Conduction in nanowires
- Optical Systems (microns)
- Random Lasers
- Microwaves (centimeters)
- Accoustical systems (meters)
- Seismic Phenomena (kilometers)

Towards a diagrammatic theory

$$\left[\nabla^2 - \frac{\varepsilon(r)}{c^2}\frac{\partial^2}{\partial t^2}\right]E(r,t) = j(r)$$

$$\left[\nabla^2 + k_+^2(1+\varepsilon(r))\right]G(r,r') = \delta(r,r')$$

Helmholtz eq. for the Green's function

$$G(r,r') = G^o(r,r') - k^2\int G^o(r,\rho)\varepsilon(\rho)G^o(\rho,r')\,d\rho \quad + k^4\int G^o(r,\rho)\varepsilon(\rho)G^o(\rho,\rho')\,\varepsilon(\rho')G^o(\rho',r')d\rho\,d\rho'$$

Dyson's solution ; $G^o(r-r')$ is the free propagator (translationally invariant) : G is not, before averaging over disorder

$$\varepsilon(r) = \sum g(r - r_i) \qquad k^4 < \varepsilon(r)\varepsilon(r') > = \Delta\delta(r,r')$$

White noise

$$G(r-r') = G^o(r-r') + \int G^o(r-\rho)\Sigma(\rho-\rho')G^o(\rho'-r')\,d\rho\,d\rho'$$

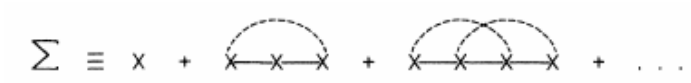

$$G(p) = \frac{1}{k^2 - p^2 - \Sigma(p)}$$

$$G(r - r') = \frac{1}{4\pi\,|r - r'|}\, Exp[ik\,|r - r'|]\, Exp\left(-\frac{|r - r'|}{2l}\right)$$

$\ell = k / \mathrm{Im}(\Sigma)$ ❄

Important Identity $\ell = 4\pi/\Delta$

$\frac{1}{kl} \equiv \frac{\mathrm{Im}(\Sigma)}{k^2}$

Is a small parameter, and the theory breaks down when it reaches 1 (Ioffe-Regel)

Diagrammatic approach to the Intensity

$$< E(r_1)E(r_2) > = < E(r_1) >< E(r_2) > + \int G\ (r_1 - \rho_1)G^*(r_2 - \rho_2)P(\rho_1, \rho_2, \rho_3, \rho_4) < E(\rho_3)E^*(\rho_4) >$$

Equation for the average intensity; BETHE-SALPETER

4-vertex insertion

At ALL orders

Each step of the ladder is of order 1

Summing the perturbation series

$$P^{(L)}(\rho_1,\rho_2,\rho_3,\rho_4) = \Delta\,\delta(\rho_1-\rho_2)\delta(\rho_3-\rho_4)\left[\delta(\rho_1-\rho_3) + \Delta\,|G(\rho_1-\rho_3)|^2 + \Delta^2\,|G(\rho_1-\rho_5)|^2|G(\rho_5-\rho_3)|^2 + \ldots\right]$$

$$1+Q(K)+Q(K)^2+Q(K)^3+\ldots \equiv \frac{1}{1-Q(K)}$$

$$Q(K) = \frac{Arc\tan(Kl)}{Kl}$$

In 3-d

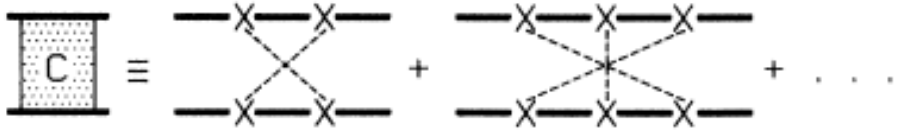

The maximally crossed diagrams (MCD) admit a similar expansion (switching around the variables)

Finally the FT of the Intensity $\langle E(r_1)E(r_2)\rangle$ becomes

$$\Gamma(K,q) = \Delta\, G\left(q+\frac{K}{2}\right) G^*\left(q-\frac{K}{2}\right)\left[\frac{1}{1-Q(K)} + \frac{Q(q+p)}{1-Q(q+p)}\right]\Gamma(K,p)$$

In the diffusive approximation

$$Q(K) \equiv 1-\frac{(Kl)^2}{3}$$

there is a diffusive pole in the insertion for I

$1/K^2$ in momentum, and $1/r$ in space

For the MCD the diffusive pole appears only for q = - p

If there is absorption the number 1 goes to

$$\frac{l_{abs}}{l_{abs}+l}$$

Universal conductance fluctuations

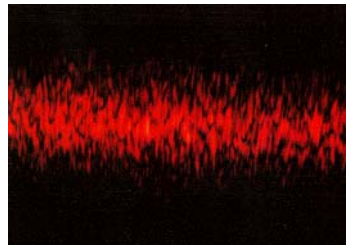

Photonic Crystals

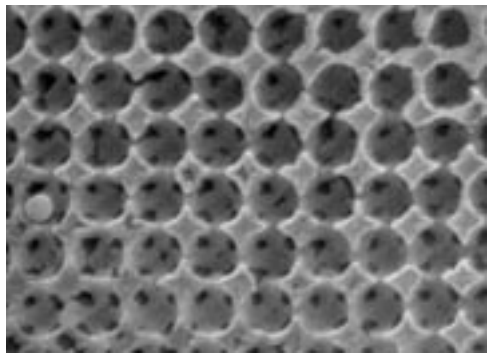

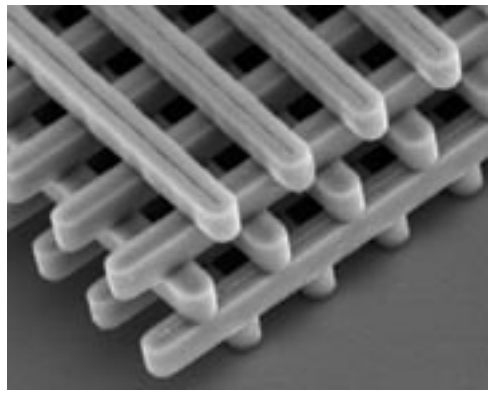

Holy Grail:

“Seeing” Localization

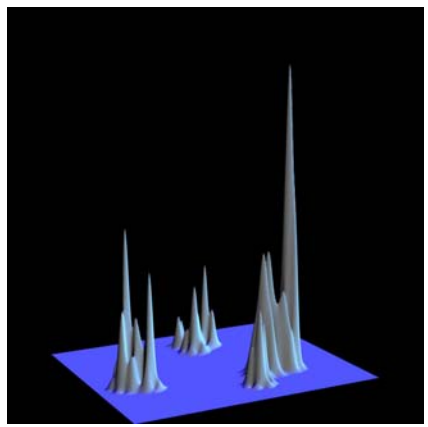

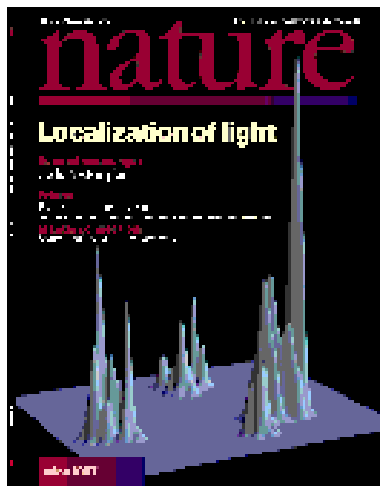

COHERENT PROPAGATION

Elastic scattering

Phase preserved

Direction randomized over ℓ

$\ell < L < l_{in}$

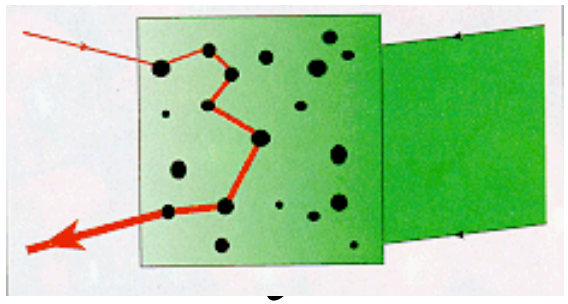

Weak Localization

Universal Conductance Fluctuations

Berkovits & Feng, *Phys Rep* 238 (1994)

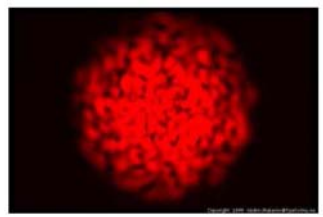

Semi-Conclusions

- A diagrammatic theory of the propagation of a wave in a disordered system, that includes all orders of scattering can be written.
- Even in its simplest version it can explain a lot of the phenomenology in the field. (WL, UCF, Memory Effects, etc)
- Can be adapted to treat polarization phenomena, anisotropy of the scatterers, more complex scatterers, etc.
- A complete systematic diagrammatic theory is still not complete

CORRELATIONS

Feng, Kane, Lee & Stone PRL 61, 834 (1988)

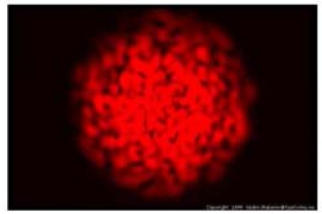

Diagrammatic theory for I - I correlations

$g = (e^2/h) \Sigma_{ab} T_{ab}$ (Landauer) $T_{ab} = | t_{ab} |^2$

Transmission: $T_a = \Sigma_b T_{ab}$; $g = \Sigma_{ab} T_{ab}$

$\langle g \rangle = N \langle T_a \rangle = N^2 \langle T_{ab} \rangle$ follows from isotropy

$$C_{aba'b'} = \langle \delta T_{ab}\, \delta T_{a'b'} \rangle = C_1 + C_2 + C_3$$

No crossing, one crossing, two crossings

prop to 1, $1/g$, $1/g^2$

C_1 is essentially $(F_E)^2$
= (square of field correlation)

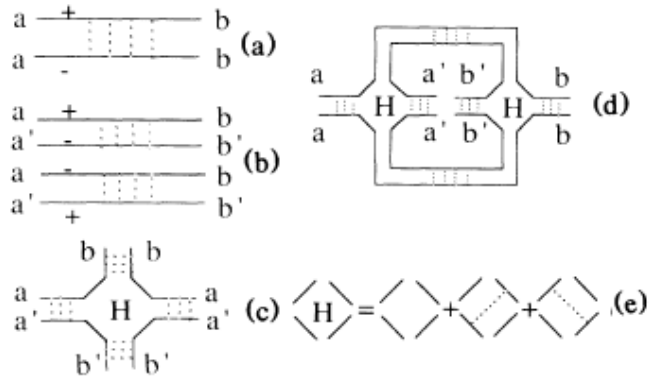

FIG. 1. (a) Feynman diagram for the average intensity $\langle T_{ab} \rangle$. (b) Diagram for $C^{(1)}_{aba'b'}$. (c) Diagram for $C^{(2)}_{aba'b'}$. (d) Diagram for $C^{(3)}_{aba'b'}$. The diamond-shaped vertex in these figures is the Hikami vertex (Ref. 16) shown in (e).

This leads to interesting experimental effects:

In transmission:

$$C_{aba'b'} = \langle T_{ab} \rangle \langle T_{a'b'} \rangle \{ C_1 \delta_{aa'} \delta_{bb'} + C_2 (\delta_{aa'} + \delta_{bb'}) + C_3 \}$$

$C_{aba'b'} = \langle Tab \rangle \langle Ta'b' \rangle \{ C_1 \underline{\Omega}_{aa'} \underline{\Omega}_{bb'} + C_2 (\underline{\Omega}_{aa'} + \underline{\Omega}_{bb'}) + C_3 \}$

$$\frac{\mathrm{var}\{T_{ab}\}}{< T_{ab} >^2} = C_{abab} = C_1 + 2C_2 + C_3$$

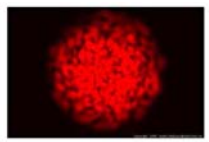

Fluctuations of the intensity at one speckle pattern (Shapiro, PRL 86)

SHORT RANGE

$$\frac{\mathrm{var}\{T_a\}}{< T_a >^2} = \sum_{b,b'} C_{abab'} = \frac{1}{N} C_1 + (1 + \frac{1}{N}) C_2 + C_3$$

Fluctuations in total transmission

(Stephen & GC, PRL 87).

LONG RANGE

$$\frac{\mathrm{var}\{g\}}{g^2} = \sum_{a,b,a',b'} C_{aba'b'} = \frac{1}{N^2} C_1 + \frac{2}{N} C_2 + C_3$$

Fluctuations in g UCF

(Feng et al, PRL88)

INFINITE RANGE

The experiment

VOLUME 88, NUMBER 12 PHYSICAL REVIEW LETTERS 25 MARCH 2002

Spatial-Field Correlation: The Building Block of Mesoscopic Fluctuations

P. Sebbah,[1] B. Hu,[2] A. Z. Genack,[2] R. Pnini,[3] and B. Shapiro[3]

[1]*Laboratoire de Physique de la Matière Condensée, Université de Nice–Sophia Antipolis, Parc Valrose, 06108, Nice Cedex 02, France*

[2]*Department of Physics, Queens College of the City University of New York, Flushing, New York 11367*

[3]*Department of Physics, Technion-Israel Institute of Technology, Haifa 32000, Israel*

(Received 16 December 2001; published 6 March 2002)

The absence of self-averaging in mesoscopic systems is a consequence of long-range intensity correlations. Microwave measurements suggest, and diagrammatic calculations confirm, that the correlation function of the normalized intensity with displacement of the source and detector, ΔR and Δr, respectively, can be expressed as the sum of three terms, with distinctive spatial dependences. Each term involves only the sum or the product of the square of the field correlation function, $F \equiv F_E^2$. The leading-order term is the product, $F(\Delta R)F(\Delta r)$; the next term is proportional to the sum, $F(\Delta R) + F(\Delta r)$; the third term is proportional to $F(\Delta R)F(\Delta r) + [F(\Delta R) + F(\Delta r)] + 1$.

DOI: 10.1103/PhysRevLett.88.123901 PACS numbers: 41.20.Jb, 05.40.–a, 71.55.Jv

Similar results in 2003-2004 for polarization

Van Tiggelen

Microwaves:

Tumbles system and averages ~ 700 configurations

Places a source at 50 positions on the input face, and detector at the output face.

Measures E(r,R)

$$C_1(\Delta r, \Delta R) = |\langle E_\nu(\vec{r},\vec{R}) E^*_{\nu'}(\vec{r}',\vec{R}')\rangle|^2 / \langle I_\nu(\vec{r},\vec{R})\rangle \times \langle I_{\nu'}(\vec{r}',\vec{R}')\rangle .$$

$$C(\Delta r, \Delta R) \equiv \langle \delta I_\nu(\vec{r},\vec{R}) \delta I_{\nu'}(\vec{r}',\vec{R}')\rangle / \langle I_\nu(\vec{r},\vec{R})\rangle \times \langle I_{\nu'}(\vec{r}',\vec{R}')\rangle ,$$

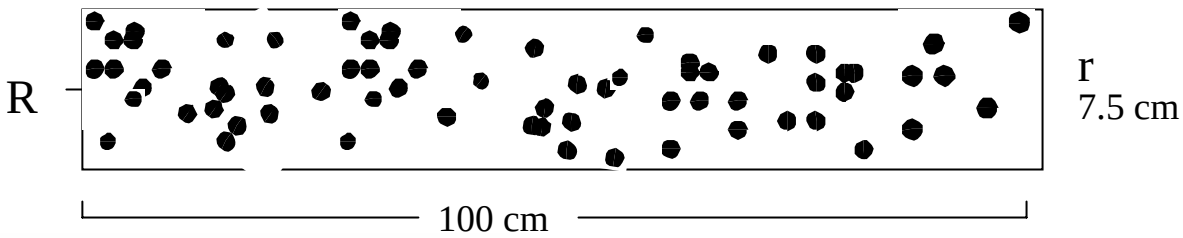

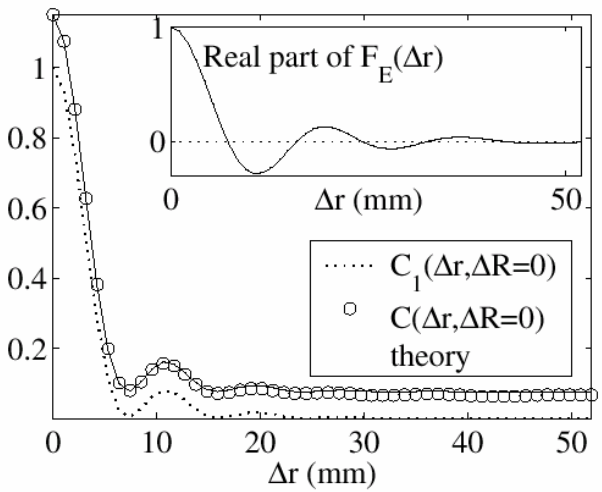

FIG. 1. Plots of $C(\Delta r, \Delta R = 0)$ and $C_1(\Delta r, \Delta R = 0)$, and theoretical fit to C. Inset: real part of the field correlation function, $F_E(\Delta r)$.

$C(\Delta r,0) = C(0,\Delta R)$

$C_1(\Delta r,0) = C_1(0,\Delta R)$

There is complete symmetry source-detector

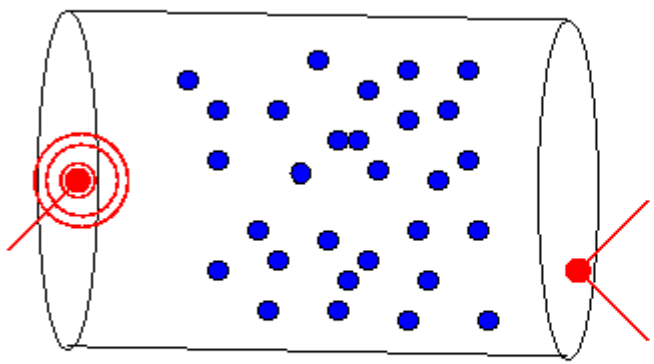

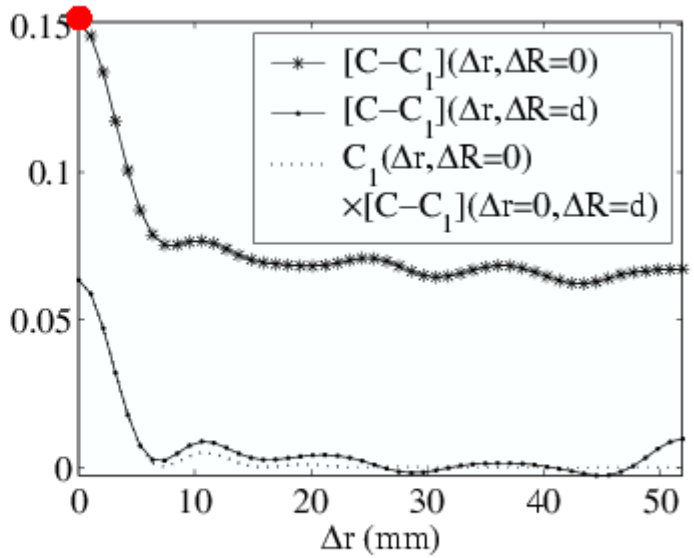

FIG. 2. Plots of $[C - C_1](\Delta r)$ for $\Delta R = 0$ and 3 cm, and $C_1(\Delta r)$ at $\Delta R = 0$.

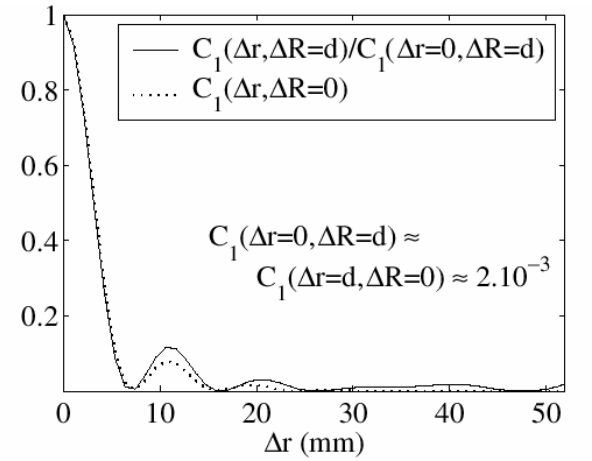

FIG. 3. Comparison of $C_1(\Delta r)$, normalized by its value at $\Delta r = 0$, for $\Delta R = 3$ cm and $C_1(\Delta r)$ at $\Delta R = 0$.

$C_1(\Delta r,d) = (0.002)\ C_1(\Delta r,0)$

C_1 is a product of two identical functions of the source and detector

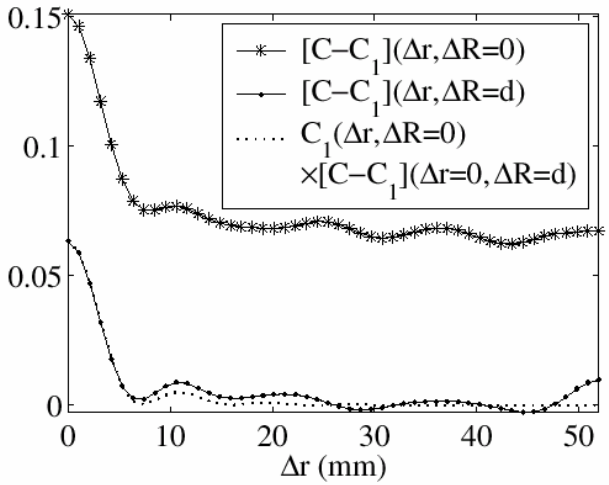

FIG. 2. Plots of $[C - C_1](\Delta r)$ for $\Delta R = 0$ and 3 cm, and $C_1(\Delta r)$ at $\Delta R = 0$.

[C- C_1](Δr, ΔR) falls to ½ when one of the variables increases beyond a certain value.

C_2 is a sum of the same two identical functions of the source and detector

THE RMT APPROACH

$$\begin{pmatrix} \mathbf{B} \\ \mathbf{A}' \end{pmatrix} = S \begin{pmatrix} \mathbf{A} \\ \mathbf{B}' \end{pmatrix} \equiv \begin{bmatrix} r & t' \\ t & r' \end{bmatrix} \begin{pmatrix} \mathbf{A} \\ \mathbf{B}' \end{pmatrix}$$

The coefficients of the scattering matrix have to verify the physical constraints

Flux conservation $S\ S^{+} = 1$

Also: $S = S^{t}$ (if there is no time reversal breaking mechanism)

Expand in eigenfunctions of the clean cavity

Quasi – 1D - geometry

$$\phi_n^{\pm}(\vec{r}) = \frac{1}{\sqrt{k_n}}\psi_n(\vec{\rho})\exp \pm ik_n z$$

Transverse Longitudinal

$$k_n = \sqrt{k^2 - q_n^2},$$

$$E(A,1) = \sum_j \left\{ \sum_a t_{ja} c_a \right\} \phi_j^+(\mathbf{r}_1)$$

$$\langle E(A,1)E^*(B,2)\rangle = \sum_{aa'jj'} c_a d_{a'}^* \phi_j^+(\mathbf{r}_1)\phi_{j'}^{+*}(\mathbf{r}_2)\langle t_{ja} t_{j'a'}^* \rangle$$

$$\langle I(A,1)I(B,2)\rangle = \sum_{aa'bb'} \sum_{ii'jj'} \{(c_a c_{a'}^*, d_b d_{b'}^*)$$

$$\times [\phi_j^+(\mathbf{r}_1)\phi_{j'}^{+*}(\mathbf{r}_1)\phi_i^+(\mathbf{r}_2)\phi_{i'}^{+*}(\mathbf{r}_2)]$$

$$\times \langle t_{ja} t_{j'a'}^*, t_{ib} t_{i'b'}^* \rangle\}.$$

Statistical averages

Key idea: maximum entropy

Transport RMT theory to evaluate the averages (Mello, Beenakker)

$$\mathbf{S} = \begin{pmatrix} \mathbf{u}^{(1)} & 0 \\ 0 & \mathbf{u}^{(2)} \end{pmatrix} \begin{pmatrix} -\sqrt{1-\tau} & \sqrt{\tau} \\ \sqrt{\tau} & \sqrt{1-\tau} \end{pmatrix} \begin{pmatrix} \mathbf{u}^{(3)} & 0 \\ 0 & \mathbf{u}^{(4)} \end{pmatrix}$$

polar decomposition

All information about transport is contained in the ♦

$$t_{ja} = \sum_n u^{(2)}_{jn} \left(\sqrt{\mathcal{T}_n}\right) u^{(1)}_{an}$$

Unitary matrices

$$\langle t_{ja} t^*_{j'a'} t_{ib} t^*_{i'b'} \rangle = \sum_{n,m,n',m'} \langle (u_{jn} u_{im})(u_{j'n'} u_{i'm'})^* \rangle^{(2)} \left(\sqrt{\mathcal{T}_n \mathcal{T}_{n'} \mathcal{T}_m \mathcal{T}_{m'}}\right) \langle (u_{an} u_{bm})(u_{a'n'} u_{b'm'})^* \rangle$$

The average over transmission coefficients factorizes in a geometric part which is independent of the transport regime ISOTROPY

One can prove results for the averages of the u^i

$\langle (u^i_{jn})(u^i_{j',n'})^* \rangle = (1/N)\, \Omega_{jj'}\, \Omega_{nn'}$

$$\langle t_{ja} t^*_{j'a'} \rangle = \frac{1}{N^2} \langle T \rangle \delta_{jj'} \delta_{aa'}$$ e.c.a

$$\langle t_{ja} t^*_{j'a'} t_{ib} t^*_{i'b'} \rangle = \left[A_N \langle T^2 \rangle - B_N \langle T_2 \rangle \right] \left(\delta_{ij'} \delta_{i'j} \delta_{ab'} \delta_{a'b} + \delta_{jj'} \delta_{ii'} \delta_{aa'} \delta_{bb'} \right) + \left[A_N \langle T_2 \rangle - B_N \langle T^2 \rangle \right] \left(\delta_{jj'} \delta_{ii'} \delta_{ab'} \delta_{a'b} + \delta_{ij'} \delta_{i'j} \delta_{aa'} \delta_{bb'} \right)$$

$$\frac{\langle I(a,1) I(b,2) \rangle}{\langle I(a,1) \rangle \langle I(b,2) \rangle} - 1 = \frac{N^4}{\langle T \rangle^2} \left[A_N \langle T^2 \rangle - B_N \langle T_2 \rangle \right] \left(|F(\vec{r}_A, \vec{r}_B)|^2 \, |F(\vec{r}_1, \vec{r}_2)|^2 \right) + \frac{N^4}{\langle T \rangle^2} \left[A_N \langle T_2 \rangle - B_N \langle T^2 \rangle \right] \left(|F(\vec{r}_1, \vec{r}_2)|^2 + |F(\vec{r}_A, \vec{r}_B)|^2 \right) + \frac{N^4}{\langle T \rangle^2} \left[A_N \langle T^2 \rangle - B_N \langle T_2 \rangle - \frac{1}{N^4} \langle T \rangle^2 \right]$$

$$|F(\vec{r}_1, \vec{r}_2)|^2 = \frac{|\Im\{G_0^+(\vec{r}_1, \vec{r}_2)\}|^2}{\Im\{G_0^+(\vec{r}_1, \vec{r}_1)\} \Im\{G_0^+(\vec{r}_2, \vec{r}_2)\}}$$

Indeed the symmetry source-detector; and the product (C_1) and the sum (C_2) have been reproduced. Also $C_3 = C_1 - 1$

$$\langle T \rangle \equiv \langle G \rangle = \sum_n \langle \mathcal{T}_n \rangle$$

$$\langle T^2 \rangle \equiv \langle G^2 \rangle$$

$$\langle T_2 \rangle = \sum_n \langle \mathcal{T}_n^2 \rangle$$

$$A_N = \frac{1 + N^2}{N^2} \frac{1}{(N^2 - 1)^2}$$

$$B_N = \frac{2}{N} \frac{1}{(N^2 - 1)^2}$$

FIELD CORRELATION

In the limit of large N

$$F(\Delta r) \rightarrow \frac{Exp[ik\Delta r]}{4\pi\Delta r}$$

Comparison between the large limit and a solution on a cavity of cross section W x W with W/(●/2) = 21/2 (which corresponds to 77 modes, similar to the experimental conditions

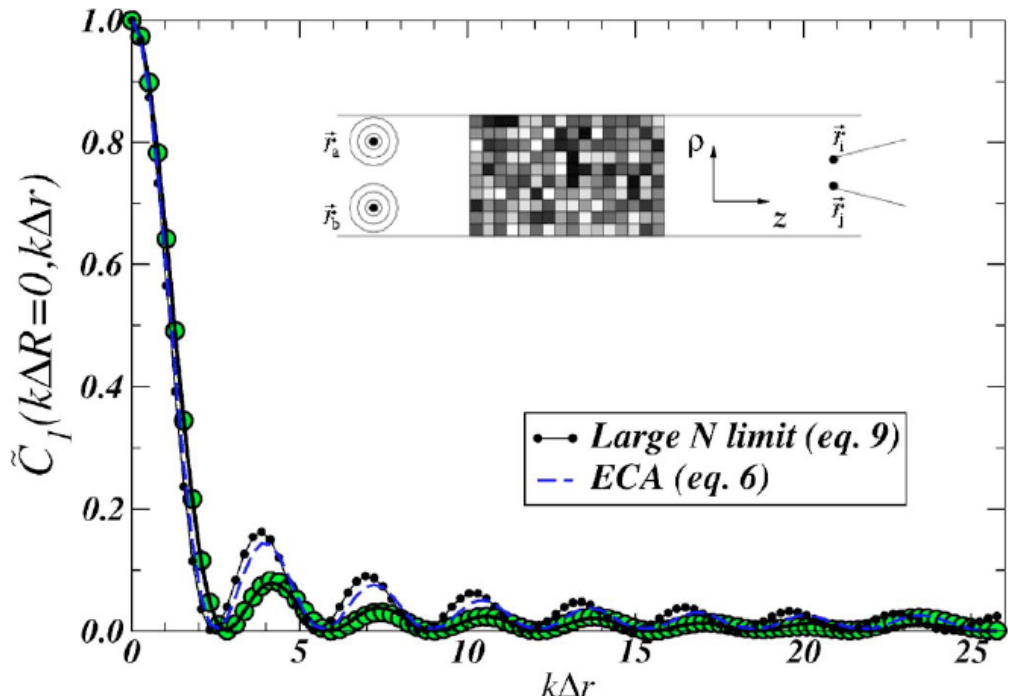

$$|F(r_1,r_2)|^2 = \frac{|\mathrm{Im}\{G_o^+(r_1,r_2)\}|^2}{\mathrm{Im}\{G_o^+(r_1,r_1)\}\,\mathrm{Im}\{G_o^+(r_2,r_2)\}}$$

$$G_o^+(r_1,r_2) = \frac{i}{2}\sum_j \Phi_j^{+*}(r_1)\,\Phi_j^+(r_2) \qquad z_2 > z_1$$

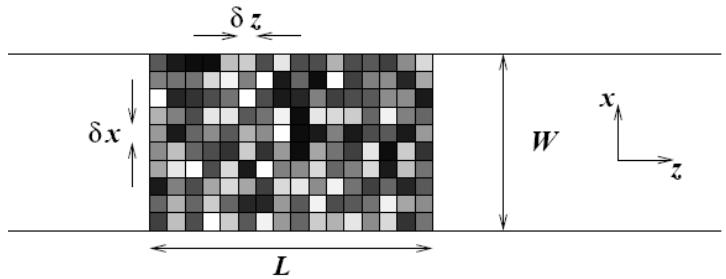

Torres and Saenz,
J.Phys. Soc. Japan **73**, 2182

Intensity correlations

$$C(\Delta\mathbf{r}_{ab},\Delta\mathbf{r}_{12}) = [|F(\mathbf{r}_a,\mathbf{r}_b)|^2|F(\mathbf{r}_1,\mathbf{r}_2)|^2]C_1 + [|F(\mathbf{r}_a,\mathbf{r}_b)|^2 + |F(\mathbf{r}_1,\mathbf{r}_2)|^2]C_2 + C_3$$

The correlations for sources at $\Delta R_{12}=0$ and $\Delta R_{12} >> \lambda$, comparing our expressions with the numerical simulation

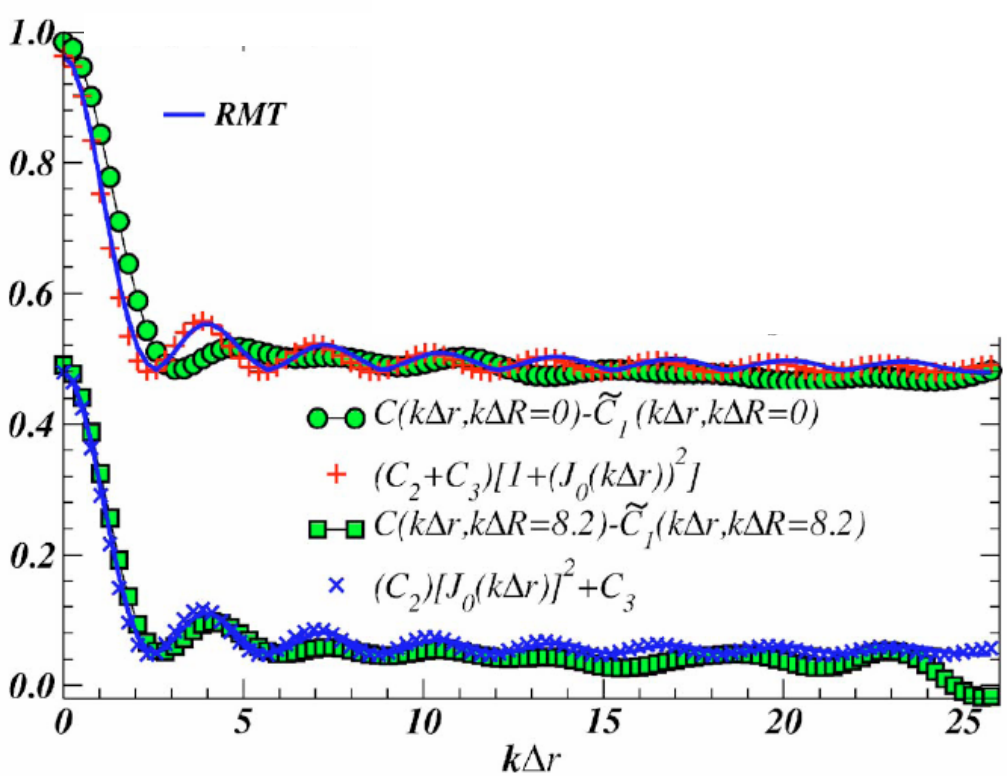

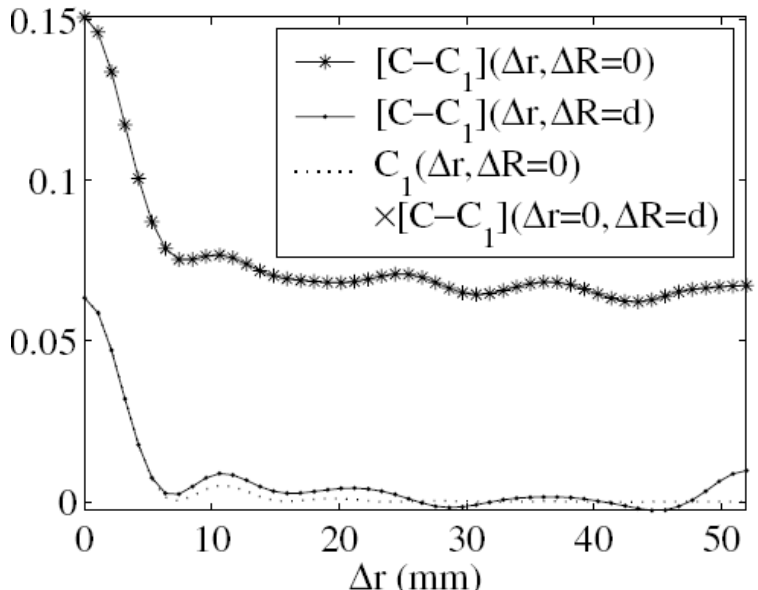

Dependence of correlations with the length of the system

Dorokhov and Mello-Pereyra-Kumar introduced an equation for the joint distribution of the transport eigenvalues τ as a function of the length s = L/ℓ (Fokker-Planck)

$$\frac{\partial P\left(\{\lambda_i\},s\right)}{\partial s}=\frac{2}{\gamma}\sum_{n=1}^{N}\frac{\partial}{\partial\lambda_n}\lambda_n\left(1+\lambda_n\right)J_\beta\left(\lambda\right)\frac{\partial}{\partial\lambda_n}P\left(\{\lambda_i\},s\right)J_\beta\left(\lambda\right)^{-1}$$

de $s\equiv L/\ell$, $\gamma\equiv\beta N+2-\beta$ y $J_\beta\left(\lambda\right)\equiv J_\beta\left(\{\lambda_i\}\right)$ se define como

$$J_\beta\left(\{\lambda_i\}\right)\equiv\prod_{n<m}\left|\lambda_m-\lambda_n\right|^\beta$$

Exact solution only for β=2 , but there are approximations in the localized case s>>N, and the diffusive limit 1<<s<<N.

$$C_1\approx 1,\ gC_2\approx 2/3 \qquad g^2C_3\approx 2/15$$

$P\left(\{x_i\},s\right)\propto\exp\left[-\beta H\left(\{x_i\},s\right)\right]$ Monte Carlo method

Froufe-Perez et al , PRL (2003)

Dependence of correlations with the length of the system

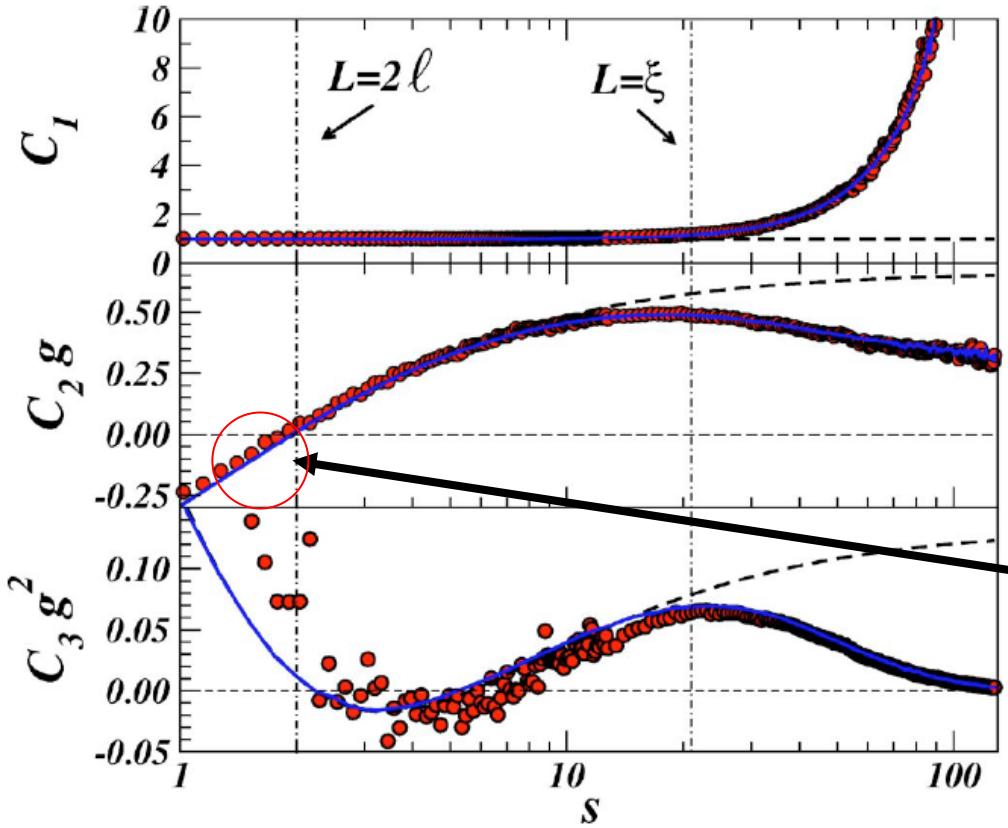

Using our numerical values for C(Δr,ΔR) we adjust with the RMT expression obtained and find C_1, C_2, C_3 at different scales

The continuous line is the DMPK solution

C_2 goes negative at small scales $s = L/\ell$

$$C\left(k\Delta R = 0, k\Delta r \simeq 25\right) \simeq C_2$$

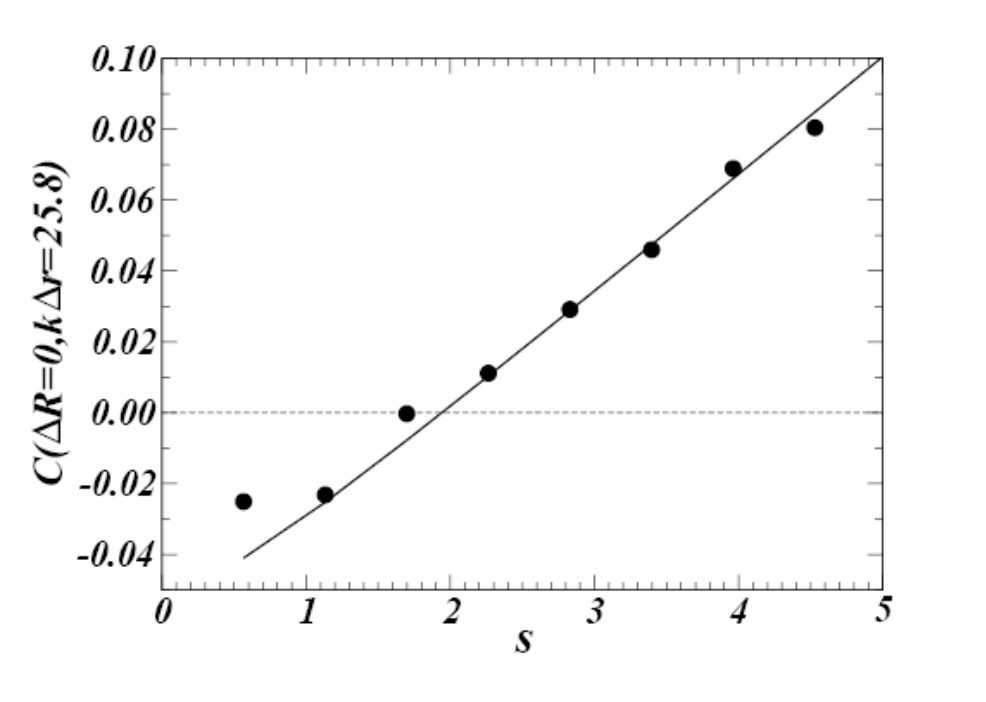

$$C_2 \simeq \frac{2}{3N} \frac{s^3 - 3s - \frac{3}{2}}{(1+s)^2}$$

Intuitive explanation in terms of flux conservation

Conclusions

- RMT is a useful tool to understand transport properties, in particular space correlations, for specific geometries.
- The structure of the correlations is independent of the transport regime.
- We get good agreement with numerical simulations.
- We can predict dependence of the correlations with length of the cavity, which can be tested.